Quaternary Relaxations in Sol−Gel Encapsulated Hemoglobin Studied via NIR and UV Spectroscopy†

Giorgio Schirò and Antonio Cupane*

CNISM and Department of Physical and Astronomical Sciences, University of Palermo, via Archirafi 36, I-90123 Palermo, Italy

Received June 13, 2007; Revised Manuscript Received July 31, 2007

ABSTRACT: In this work, we study the kinetics of the R → T transition in hemoglobin using a combination of near-infrared and near-ultraviolet spectroscopy. We use a sol−gel encapsulation protocol to decelerate the conformational transitions and to avoid spectral perturbations arising from ligand migration and recombination. We monitor two spectroscopic markers: band III in the near-IR, which is a fine probe of the heme pocket conformation, and the tryptophan band in the near-UV, which probes the formation of the Trpβ37−Aspα94 hydrogen bond, characteristic of the T structure, at the critical $\alpha_1\beta_2$ subunit interface. The time evolution of these two bands is monitored after deoxygenation of encapsulated oxyhemoglobin, obtained by diffusion of a reducing agent into the porous silica matrix. Characteristic spectral shifts are observed: comparison with myoglobin enables us to assign them to quaternary structure relaxations. Band III spectral relaxation is clearly nonexponential, and analysis with the Maximum Entropy Method enables us to identify three processes. On the other hand, near-UV spectral relaxation follows an exponential decay with a time constant closely corresponding to the second process observed in the near IR. Very interestingly, the rates of all processes markedly depend on the viscosity of the co-encapsulated solvent, following a power law. Our results reveal correlations between heme pocket relaxations, induced by the R → T transition, and structural event(s) occurring at the $\alpha_1\beta_2$ interface and highlight their solvent dependence. The power law viscosity dependence of relaxation rates suggests that the observed protein relaxations are "slaved" to the co-encapsulated solvent. The stepwise character of the quaternary transition is also evidenced.

Conformational transitions involving the quaternary structure of proteins are fundamental for several biological mechanisms. The R → T transition of hemoglobin, in particular, is strictly related to the highly cooperative behavior of this protein in its reaction with oxygen. In fact, cooperativity in ligand binding arises from a ligation-controlled quaternary structure switch from a low-affinity state to a high-affinity state (*1*). The end points of the hemoglobin quaternary transition have been characterized well: they correspond to the crystal structures of HbCO[1] (*2*) (high-affinity state, R or R_2 quaternary conformation)[2] and of deoxyHb (low-affinity state, T quaternary conformation) (*3*). On the basis of the crystal structures mentioned above, the R → T conformational transition can be described as a relative motion between the two $\alpha\beta$ dimers corresponding to a rotation of ≈15° and a translation of ≈0.8 Å (*6*, *7*); as a consequence, the two quaternary structures are characterized by different geometries for the interdimer contacts and different arrangements of hydrogen bonds and salt bridges.

Much less is known about the structural pathway connecting the end states of the allosteric transition in Hb, although recently several approaches, both experimental (*8*−*13*) and computational (*14*, *15*), provided additional information. In particular, there is a continuing debate between the "standard" description of the R → T switch as a single-step concerted transition (*16*−*18*) and the more complex description as a multistep compound pathway involving several intermediates (*9*−*13*); in any case, a complete and well-accepted picture is at the moment far from being reached.

The hydration properties of hemoglobin in R and T quaternary conformations are also known to be widely different; in particular, it has been shown that ∼60 water molecules are released at the R → T transition (*19*, *20*) so that T-state Hb is dehydrated with respect to R-state Hb. A marked effect of solvent composition on the T ↔ R allosteric equilibrium of Hb is therefore expected and, in fact, measured (*21*, *22*). Analogous studies on the effect of solvent viscosity on the rates of conformational transitions have also been performed for both myoglobin (*23*) and hemoglobin (*24*); such studies are greatly relevant also in view of the dependence of protein dynamics upon the dynamics of the solvent in the hydration shell (*25*).

† This work has been supported by a grant from Italian MIUR (PRIN 2005, 2005027011).

* To whom correspondence should be addressed: Department of Physical and Astronomical Sciences, University of Palermo, Via Archirafi 36, I-90123 Palermo, Italy. Telephone: +39-(0)91-6234221. Fax: +39-(0)91-6162461. E-mail: cupane@fisica.unipa.it.

[1] Abbreviations: Hb, hemoglobin; HbCO, carbonmonoxyhemoglobin; deoxyHb, deoxyhemoglobin; HbO_2, oxyhemoglobin; TMOS, tetramethylorthosilicate; MEM, Maximum Entropy Method.

[2] Two different quaternary structures have been found for HbCO depending on the crystallization procedure: the high-salt R structure (*2*) and the low-salt R_2 structure (*4*). Recently published NMR data (*5*) suggest that the quaternary structure of HbCO in solution is actually a nearly 50% mixture of R and R_2 in dynamical equilibrium.

10.1021/bi701166m CCC: $37.00
Published on Web 09/19/2007

A large body of experimental data on the kinetics of the R → T transition in Hb has been obtained with the flash-photolysis technique. In these experiments, a HbCO sample is illuminated by an "instantaneous" laser flash that breaks the iron−ligand bond. The subsequent transient spectral changes, reflecting structural changes in the protein and/or ligand migration and recombination, are monitored with time-resolved spectroscopy. Results obtained with optical absorption (Soret band) (*8*, *10*, *12*, *16*, *26*) substantially converge to identify five (or six) different relaxations on time scales ranging from nanosecond to millisecond. These relaxations are interpreted as corresponding to ligand rebinding and tertiary and quaternary conformational changes; the spectral relaxation occurring at ∼20 μs is usually attributed to the R → T transition. Earlier processes, occurring on the nanosecond to microsecond time scale, are attributed to geminate rebinding and to tertiary structure changes; late events on the time scale of hundreds of microseconds and milliseconds depend on the CO concentration and are therefore attributed to the bimolecular rebinding of CO from the solution to R-state and T-state hemoglobin tetramers, respectively. This picture is in substantial agreement with data obtained with time-resolved resonance Raman spectroscopy (*27*, *28*).

The recent development of flash photolysis in connection with time-resolved vibrational spectroscopy [both FTIR (*29*) and UVRR (*12*, *13*, *30*)] and with time-resolved CD (*9*) and MCD (*11*, *31*) spectroscopy has provided new insights and added to the complexity; in fact, further spectroscopic intermediates on the submicrosecond time scale have been evidenced and attributed to multiple intermediate structures in a multistep compound pathway of the allosteric transition. In recent papers (*12*, *13*), the group of T. Spiro has proposed a "working model" for a multistep allosteric transition pathway. After photolysis, the breaking of the Fe−CO bond brings the protein into the so-called geminate state: strain first accumulates at the heme−imidazole complex and subsequently (∼65 ns) relaxes via the rotation of the E and F helices in which hydrogen bonds connecting different helices are broken. In the following steps, these bonds are re-established (∼740 ns), the hydrogen bond between Trpβ37 and Aspα94 is formed (the so-called "hinge contact", ∼2.9 μs), and finally the formation of a hydrogen bond between Tyrα42 and Aspβ99 (the so-called "switch contact", ∼21 μs) concludes the transition toward the T state, this last step corresponding to the classical R → T transition, as detected by optical spectroscopy.

In flash photolysis experiments, however, spectral signals arising from conformational transitions are always superimposed with those (often much larger) arising from ligand rebinding; this problem frequently makes the quantification, or even the detection, of the structure-dependent spectral contributions very difficult. As far as time-resolved spectroscopic investigations of the hemoglobin R → T transition are concerned, removal of any effect linked to ligand rebinding seems therefore highly desirable.

For this work, we adopted the technique of sol−gel encapsulation. The basic idea is rather simple. Following a well-established approach (*32*), HbO_2 (in the quaternary R or R_2 conformation) is encapsulated in a porous silica hydrogel obtained through the hydrolysis and polycondensation of the alkoxide precursor TMOS. Several spectroscopic and functional studies (*32*−*34*) show that encapsulated proteins maintain almost intact spectral and functional properties with respect to the solution, thus indicating that the encapsulation procedure per se does not introduce relevant structural distortions. On the other hand, a number of data obtained with both optical (*33*, *35*−37) and resonance Raman spectroscopy (*38*, *39*) show that rates of conformational transitions in encapsulated proteins can be substantially reduced. In particular, for sol−gel-encapsulated Hb, it has been shown that the rate of the R → T quaternary structural transition is dramatically reduced to days, weeks, or even years, the extent of the slowing depending on details of the encapsulation protocol, temperature, and solvent composition. Once HbO_2 is encapsulated, the ligand can be removed by diffusing a reducing agent (sodium dithionite). Due to matrix porosity, the dithionite diffusion time can be made much faster than the characteristic times of the quaternary transition of sol−gel-encapsulated Hb: the protein is "instantaneously" deoxygenated while its quaternary structure remains (initially) R. This makes it possible, once suitable spectroscopic markers are chosen, to follow the kinetics of conformational transitions using conventional absorption spectroscopy (time resolution of ∼100 s) and preventing any interference from ligand rebinding. Moreover, in view of the high porosity of the sol−gel matrix, the composition of the solvent co-encapsulated with the protein within the matrix pores can be easily varied, thus allowing studies at various solvent compositions.

We have chosen two spectroscopic markers that probe two different sites in the protein: the so-called band III in the near-infrared region and the band at ≈290 nm in the near-ultraviolet absorption region of aromatic residues.

Band III, positioned at ∼760 nm (∼13200 cm^{-1}), is observed only in the deoxygenated derivative of Hb and is attributed to a porphyrin to iron charge transfer electronic transition (*40*). It is mainly sensitive to heme pocket structural relaxations, and for this reason, it was called the "conformation band". It was shown (*41*−*43*) that, in the 10 ns photoproduct obtained after photolysis of HbCO, band III is red-shifted by ∼6 nm (∼120 cm^{-1}) from its equilibrium position; in the pioneering work of Sassaroli and Rousseau (*41*), spectral relaxation toward the equilibrium deoxy position was observed at up to 10−20 μs where a plateau region was reached with a residual red shift of ∼2 nm (∼35 cm^{-1}). Ligand recombination prevented meaningful measurements at longer delay times. In our previous work on the identification of spectroscopic markers of the R → T transition in sol−gel-encapsulated Hb (*34*), the residual shift described above was clearly assigned to the quaternary structure transition. Band III therefore appears to be a suitable probe for studying the effects of protein conformational relaxations (both tertiary and quaternary) as seen in the active site (heme pocket) of the protein.

The band at ∼291 nm (∼34350 cm^{-1}) is assigned to the tryptophanyl residues of the protein; the band red shift observed in deoxyHb − oxyHb difference spectra has been specifically attributed by Perutz et al. (*44*, *45*) to Trpβ37 located at the quaternary structure sensitive $\alpha_1\beta_2$ interface. In fact, these authors showed that this band shift is not present in a mutant hemoglobin with a Trpβ37 → Ser substitution and clarified that the peak shift observed for this band

between liganded and unliganded hemoglobin is related only to the quaternary structure change and not to the ligation state: the observed shift was assigned to a perturbation in the Trpβ37 electronic structure induced by formation of the Trpβ37−Aspα94 hydrogen bond, characteristic of the T structure. This assignment was questioned in the works by Peterson and Friedman (*46*) and Kiger et al. (*47*) showing that mutation of Trpβ37 to Tyr, Ala, Gly, or Glu induces a large perturbation in the $\alpha_1\beta_2$ interface and leads to dissociation of the tetramer into dimers. However, more recently, Goldbeck et al. (*11*) have used near-UV time-resolved magnetic circular dichroism spectroscopy to follow the Trpβ37 band position during the R → T transition in native Hb: they found that the peak of the tryptophan band red-shifted rapidly from its R-state position by ∼0.6 nm with a time constant of ∼2 μs. This was attributed to the formation of the hinge contact Trpβ37−Aspα94 hydrogen bond, in agreement with the time-resolved resonance Raman data of Spiro and co-workers (*12*). The ∼291 nm band appears therefore to be a suitable probe for studying the protein quaternary relaxation, as seen by the crucial $\alpha_1\beta_2$ intersubunit interface.

MATERIALS AND METHODS

Samples

Hemoglobin was prepared from the blood of a single healthy individual following a standard procedure described previously (*48*). Concentrated (∼30% by weight) hemoglobin stocks were stored in liquid nitrogen as the oxy form; suitable aliquots were thawed immediately before use. Lyophilized myoglobin from horse heart was purchased from Sigma Aldrich.

Protein encapsulation in silica hydrogels was performed using the following protocol. A solution containing 60% TMOS, 38% water, and 2% HCl (0.04 M) (solution A) was sonicated for 20 min in an ice bath; immediately after sonication, it was mixed in a 3:2 proportion and at 7 °C with a second solution (solution B) containing the protein at a suitable concentration, glycerol [53.3% (v/v) in water], and 0.2 M potassium phosphate buffer (pH 7). Under these conditions, formation of a solid, jelly-like hydrogel occurred in ∼1 min. After gelification, the sample was covered with a protective solution [40% (v/v) glycerol and 0.2 M potassium phosphate buffer (pH 7)] and left to age for 10 h, at ∼7 °C. This procedure was followed for all samples so that hemoglobin (or myoglobin) was encapsulated in a silica hydrogel matrix formed under standard and reproducible conditions. After 10 h, the protective solution was substituted with an otherwise identical solution containing the desired glycerol:water proportion in the range of 0−70% (v/v) so that the solvent composition inside the hydrogel could be varied. Equilibration of the hydrogel with the new solvent was performed overnight at 7 °C; the protective solution was changed at least three times during this period. The effective sample equilibration with the protective solution was checked by measuring the relative intensities of glycerol and water IR absorption bands. Given our sol−gel protocol, both glycerol [and/or water/glycerol aggregates (*49*)] and hemoglobin−hydration shell act as templates directing the formation of the silica cages and network: this provides the proteins not only with numerous access channels for the reactants but also with ample surrounding space for accommodation of solvent. Pore size estimates in analogous sol−gel silica matrices obtained using fructose and horseradish peroxidase as templates [measured from N_2 desorption isotherms via the Barret−Joyner−Halenda (BJH) approach] give rather broad distributions with, however, a dominant contribution of "mesopores" with an ≈35−45 Å BJH pore diameter (*50*, *51*). This suggests that at most one protein molecule (plus solvent) is present in one matrix pore; moreover, given the high protein concentration at the moment of encapsulation (see below), the fraction of hemoglobin dimers can be considered negligible.

To perform NIR and near-UV measurements, from this common recipe two analogous samples were prepared with suitable characteristics for the different spectral regions.

Samples for NIR Measurements. Protein solution B contained 5.5 mM (in heme) HbO_2 or MbO_2; after protein solution B had been mixed with solution A, the resulting mixture was layered on the inner face of a PMMA cuvette. The gel thickness was ∼1 mm. Immediately before the experiment, the protective solution was anaerobically substituted with an otherwise identical solution saturated with N_2 and containing 50 mM sodium dithionite; this procedure defined time zero for the kinetic measurements.

Samples for Near-UV Measurements. Protein solution B contained 1.4 mM (in heme) HbO_2; after solution B had been mixed with solution A, the resulting mixture was injected into a rotating glass tube. The resulting gel thickness was ∼100 μm. As for the previous sample, immediately before the experiment the protective solution was anaerobically substituted with an otherwise identical solution saturated with N_2 and containing 10 mM sodium dithionite. Hemoglobin reduction occurred in ∼1 min in view of the small gel thickness and was checked by inspection of the visible spectrum. After full reduction, the protective solution was anaerobically substituted with a new one, fully N_2 saturated and sodium dithionite free; this last procedure, necessary since dithionite absorption in the near-UV region would obscure the hemoglobin absorption, defined time zero for the kinetic measurements.

In all samples, the percentage of methemoglobin was found to be less than 5%, as judged from spectral inspection. For the more concentrated HbO_2 or MbO_2 samples used for band III studies, the percentage of methemoglobin was estimated from the ratio of OD_{630} to OD_{800} (∼0.5 and 10 for oxy and met proteins, respectively); the absence of significant protein oxidation during the kinetics was checked via the absorbance at 800 nm (nearly isosbestic for oxy and deoxy proteins).

Spectral Measurements

Absorption spectra in the near-UV and NIR regions were recorded with a Jasco V-570 spectrophotometer. The spectral resolution was 0.2 nm for UV spectra and 1 nm for NIR spectra. The background was subtracted from the spectra via a cubic baseline. The temperature was set to 25 °C and controlled to within ±0.1 °C with a Peltier thermostat.

MEM analysis has been performed with MemExp, version 3.0, developed by P. J. Steinbach and available on-line. Details of the algorithm adopted in the program have been discussed in the literature (*52*, *53*).

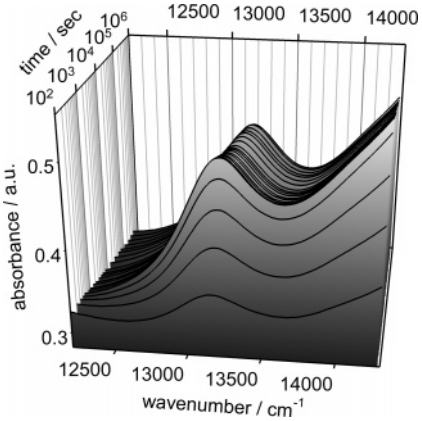

FIGURE 1: Time evolution of band III. The data are for a sample of HbO_2 encapsulated in a silica hydrogel; the co-encapsulated solvent is 20% (v/v) glycerol/water. $T = 25$ °C.

As usual, the zeroth, first, and second moments of the bands are defined as

$$M_0 = \int_{-\infty}^{+\infty} A(\nu)\, d\nu$$

$$M_1 = \frac{\int_{-\infty}^{+\infty} \nu A(\nu)\, d\nu}{M_0}$$

$$M_2 = \frac{\int_{-\infty}^{+\infty} \nu^2 A(\nu)\, d\nu}{M_0} - M_1^2$$

RESULTS AND DISCUSSION

Band III Spectral Relaxation. Typical experimental data concerning the time evolution of band III are reported in Figure 1. As Figure 1 shows, band III gradually develops following sample deoxygenation; further band shifts are then observed after longer times while the band intensity remains almost constant. The time dependence of the zeroth, first, and second moments of the band in typical experiments is reported in panels a−c of Figure 2, respectively. Two kinetic processes are observed: (1) an almost exponential M_0 increase with M_1 remaining at the value typical of R-state deoxyHb encapsulated in a silica hydrogel (*34*) and (2) a clearly nonexponential M_1 shift, occurring at an almost constant M_0, toward the equilibrium value observed for deoxyHb in solution or for T-state deoxyHb encapsulated in a silica hydrogel (*34*). During the entire time course of the experiment, the second moment of the band exhibits only a very small increase.

The first process can clearly be attributed to the diffusion of dithionite inside the silica gel and to sample deoxygenation; full deoxygenation was checked in a separate experiment on a less concentrated sample by looking at the full development of the deoxy visible band at ≈555 nm. It is remarkable that this first process appears to be rather well separated in time from the second one, even at the highest glycerol concentration (i.e., at the highest solvent viscosity) studied: this enables us to study spectral shifts linked to protein conformation without interference from variations of the ligation state.

The second process is much slower and occurs on a time scale from thousands of seconds to several days or even

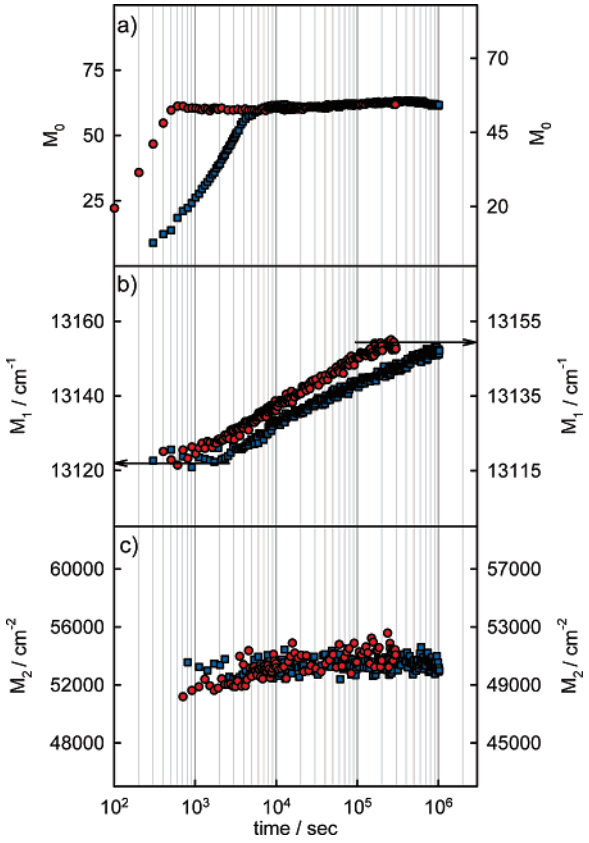

FIGURE 2: (a) Time evolution of the band III zeroth moment. (b) Time evolution of the band III first moment. The arrows indicate M_1 values relative to R-state (left arrow) and T-state deoxyHb (right arrow) encapsulated in a silica hydrogel under the same experimental conditions. (c) Time evolution of the band III second moment. The data are for HbO_2 samples encapsulated in a silica hydrogel at two different compositions of co-encapsulated solvent: 20% (v/v) glycerol/water (red circles, left axis) and 70% (v/v) glycerol/water (blue squares, right axis). $T = 25$ °C.

weeks, depending on solvent composition; it spans an overall M_1 shift of ∼35 cm^{-1}, starting from an M_1 value characteristic of deoxyHb encapsulated in a silica hydrogel in the R quaternary conformation and ending with an M_1 value characteristic of deoxyHb encapsulated in a silica hydrogel in the T quaternary conformation and to deoxyHb in solution (arrows in Figure 2b; *34*). In the room-temperature flash photolysis study of HbCO by Sassaroli and Rousseau (*41*), band III relative to the 10 ns photoproduct was found to be red-shifted by ∼120 cm^{-1} from the equilibrium deoxyHb value; the time-dependent relaxation of the peak position showed a large change between 10^{-8} and 10^{-6} s, followed by a plateau region extending up to 10^{-5} s with a remaining red shift of 30−40 cm^{-1}. Meaningful measurements at longer delay times were prevented by ligand recombination. The authors attributed the observed peak shift to relaxation(s) of the tertiary structure, while the residual red shift was assigned to the effect of the quaternary conformation. It is remarkable that the total M_1 span observed in our experiments (∼35 cm^{-1}) matches exactly the residual red shift reported by Sassaroli and Rousseau (*41*); we are therefore led to assign the M_1 shift observed in our experiments to the effect of the R → T quaternary transition. The assignment described above is further substantiated by the data reported in Figure 3a−c, obtained with sol−gel-encapsulated myoglobin. In fact, for myoglobin, the first process (M_0 increase due to dithionite

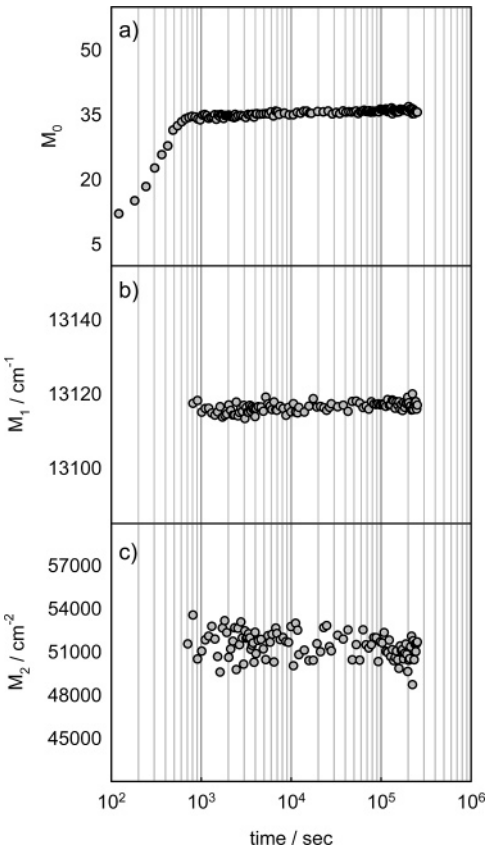

FIGURE 3: Same as Figure 2, for myoglobin. The data are for a sample of MbO_2 encapsulated in silica hydrogel; the co-encapsulated solvent is 20% (v/v) glycerol/water. $T = 25$ °C.

diffusion and protein deoxygenation) is again observed and is identical to that relative to Hb; different is the fact that no M_1 shift was observed over the entire time interval that was investigated, the observed constant M_1 value being equal to that relative to equilibrium deoxy Mb in solution. It should be noted that the 10 ps photoproduct obtained after flash photolysis of MbCO in solution and at room temperature exhibits a band III red shift of ~100 cm^{-1} with respect to the equilibrium deoxy value (*54*, *55*); spectral relaxation is observed on a time scale of picoseconds to nanoseconds.

Comparing data in Figures 2 and 3 with data from flash photolysis studies in solution, we conclude that in our sol−gel encapsulated samples tertiary relaxations remain faster than the time resolution of our experiments ($>10^2$ s, limited by dithionite diffusion times) and are therefore not detectable. Previous work by J. Friedman and co-workers on the time evolution of the iron−proximal histidine stretching frequency showed that the sol−gel was indeed able to substantially decelerate the hemoglobin tertiary relaxations and therefore to trap R-state tertiary structure intermediates (*38*); as Figures 2 and 3 show, this is not observed in our work, the difference being attributable to the different sol−gel encapsulation protocols. On the contrary, rates of quaternary relaxation(s) are reduced to fall within our time window; it is remarkable that sol−gel encapsulation is able to increase the characteristic times of quaternary relaxation(s) in hemoglobin by some 9 orders of magnitude, from the value of ~10^{-5} s observed in solution (*16*) to the value of ~10^4 s observed in our experiment.

We stress two further features of the data in Figures 2 and 3:

(a) Both for Hb and for Mb, the M_1 deoxy equilibrium values observed in sol−gel-encapsulated samples coincide with those observed in solution; this indicates that our sol−gel encapsulation protocol does not introduce any relevant (or, at least, spectrally detectable) structural distortions in the encapsulated proteins. (b) For Hb, the M_1 shift induced by the R → T quaternary transition occurs without any relevant M_0 variation; in view of the charge transfer character of band III (*40*, *56*), this indicates that the R → T transition of deoxyHb does not involve any further displacement of the iron from the heme plane, contrary to previous suggestions in the literature (*57*).

To analyze quantitatively the observed spectral shifts, we define a relaxation function as follows:

$$\Phi(t) = \frac{M_1(t) - M_1(\infty)}{M_1(0) - M_1(\infty)}$$

According to its definition, $\Phi(t)$ represents the fraction of hemoglobin molecules that, at a time t after deoxygenation, are still in the R quaternary conformation. In view of the clear nonexponential character of the relaxation, we have analyzed the data with the Maximum Entropy Method (MEM) (*52*, *53*). This method assumes that the kinetics is described by a distribution of relaxation processes each having a different lifetime and extracts the most probable lifetime distribution, $g(\tau)$.

Figure 4 reports the $\Phi(t)$ values measured for all our samples together with the $g(\tau)$ distributions obtained from the MEM analysis. From Figure 4 the following facts emerge.

First, under all the conditions that were studied, $g(\tau)$ is composed of three very narrow peaks. This implies that the overall band III relaxation reflects three (maybe slightly distributed) processes[3] rather than a single heterogeneous relaxation. Second, the characteristic times of the three processes depend markedly on the composition of the solvent inside the pores of the matrix, the difference between the 0 and 70% glycerol/water proportions being a factor of ~5. On the other hand, the amplitudes of the three processes are largely solvent independent (see Table 1).

With regard to the first point, we note that, in principle, the observed result could also be attributed to the existence of a single relaxation process performed by three different protein structures (i.e., three different conformations of HbO_2 and/or three different environments inside the silica matrix)

[3] In our experiment, time zero corresponds to the time at which the sample is deoxygenated. In view of the finite time that it takes for sodium dithionite to diffuse into the silica matrix, a spreading of zero times occurs, and one may wonder how this effect influences the observed relaxations. From Figure 2a, it can be seen that the deoxygenation kinetics (measured from the M_0 time dependence) is almost exponential and that its rate (k_0) is at least 1 order of magnitude faster than the M_1 relaxation (compare panels a and b of Figure 2). It can be easily shown that under the assumption of exponential deoxygenation where $k_0 \gg k_I$ (i.e., deoxygenation process much faster than spectral relaxations) $M_1(t)$ approaches the value obtained when all hemoglobin molecules are deoxygenated at the same time. Moreover, taking into account an exponential distribution of deoxygenation times brings about in the $\Phi(t)$ time dependence a further exponential term with a rate constant equal to k_0; fittings performed with such a new term gave almost indistinguishable results. We therefore conclude that rates of the relaxation processes extracted from the M_1 time dependence are, under our experimental conditions, not affected by the time distribution of hemoglobin deoxygenation.

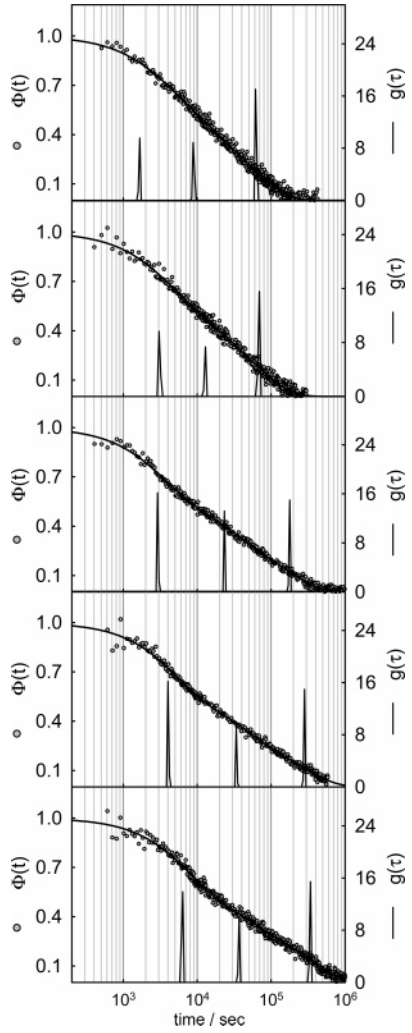

FIGURE 4: Time evolution of the relaxation function $\Phi(t)$ for various HbO_2 samples encapsulated in a silica hydrogel with different "solvent" conditions. The $g(\tau)$ distributions and the fittings obtained with the MEM analysis are also reported (right scale and solid lines). Glycerol/water proportions (v/v) are, from top to bottom 0, 20, 40, 50, and 70%.

each having a different lifetime. We discard this possibility for the following reasons: different quaternary structures for HbO_2 have never been crystallized or observed in solution; analogous data obtained in the near-UV spectral region reveal a single relaxation; and distinct encapsulation environments within the same hydrogel do not correspond to a realistic picture of matrix structure since the structural heterogeneity of matrix pores should correspond to a broad distribution rather than a discrete number of different environments. Moreover, previous kinetic studies on sol−gel-encapsulated Hb using Soret band absorption spectroscopy have shown the existence of monophasic processes occurring in encapsulated Hb (*35*) and demonstrated that the R → T transition in gel-encapsulated Hb at 20 °C can be described well by three kinetic components of nearly equal amplitudes and time constants of $\sim 8 \times 10^2$, $\sim 5.4 \times 10^3$, and $\sim 6.8 \times 10^4$ s, respectively. Our results are in fairly good agreement with those in ref *35*, thus suggesting that the same kinetic processes are monitored with Soret band and NIR band III absorption spectroscopy; the slight discrepancies can be attributed to the different temperature or, more likely, the different encapsulation protocols used. In view of the considerations mentioned above, we conclude that data in Figure 4 can be taken as further evidence of a multistep pathway for the R → T allosteric transition in hemoglobin.

With regard to the second point, we stress that, as pointed out in Materials and Methods, in all our samples the hydrogel matrix that encapsulates the protein is always formed under identical conditions and the solvent is varied only after the gel is well-stabilized. The dependence of relaxation rates on solvent composition therefore suggests that the 9 order of magnitude effect of sol−gel encapsulation on R → T transition rates is attributable not only to covalent, van der Vaals, or electrostatic contacts between protein residues and functional groups on the pore surfaces but also to interactions between the protein and the solvent within the confined geometry provided by the hydrogel matrix. To highlight this effect, we report in Figure 5 the dependence of relaxation rates ($k = 1/\tau$) upon bulk solvent viscosity, on a logarithmic scale. Linear relationships are found for all processes, in agreement with previously published results (*24*, *58*); values of slopes are 0.35, 0.44, and 0.54 for processes I, II, and III, respectively, in remarkable agreement with the value of 0.55 found by different authors in different systems (*58*, *59*). A power law dependence of relaxation rates upon bulk solvent viscosity ($k \propto \eta^{-p}$) is consistent with the "slaving model" of Frauenfelder and co-workers (*25*, *59*−*61*) and suggests that hemoglobin quaternary relaxation(s) follows the α-relaxation in the solvent. The fractional viscosity dependence ($p < 1$) can be attributed to a preferential hydration effect (see, for example, ref *62* and references cited therein) and/or to a solvent-dependent entropy term (*59*).

Table 1: Solvent Dependence of Characteristic Times and Amplitudes of the Various Processes Observed in the Relaxation of Band III

glycerol/water (v/v)	τ_I (s)	τ_{II} (s)	τ_{III} (s)
0%	$(1.7 \pm 0.1) \times 10^3$	$(8.9 \pm 0.3) \times 10^3$	$(6.3 \pm 0.3) \times 10^4$
20%	$(3.1 \pm 0.2) \times 10^3$	$(12.9 \pm 0.7) \times 10^3$	$(6.9 \pm 0.3) \times 10^4$
40%	$(3.0 \pm 0.1) \times 10^3$	$(24.0 \pm 1.2) \times 10^3$	$(17.1 \pm 0.7) \times 10^4$
50%	$(4.0 \pm 0.2) \times 10^3$	$(33.4 \pm 1.2) \times 10^3$	$(27.5 \pm 1.3) \times 10^4$
70%	$(6.3 \pm 0.3) \times 10^3$	$(38.2 \pm 1.7) \times 10^3$	$(34.1 \pm 1.7) \times 10^4$

glycerol/water (v/v)	amplitude I	amplitude II	amplitude III
0%	0.41 ± 0.02	0.23 ± 0.02	0.36 ± 0.03
20%	0.42 ± 0.02	0.22 ± 0.03	0.36 ± 0.02
40%	0.40 ± 0.01	0.25 ± 0.02	0.35 ± 0.01
50%	0.41 ± 0.01	0.27 ± 0.02	0.32 ± 0.02
70%	0.40 ± 0.02	0.23 ± 0.01	0.37 ± 0.03

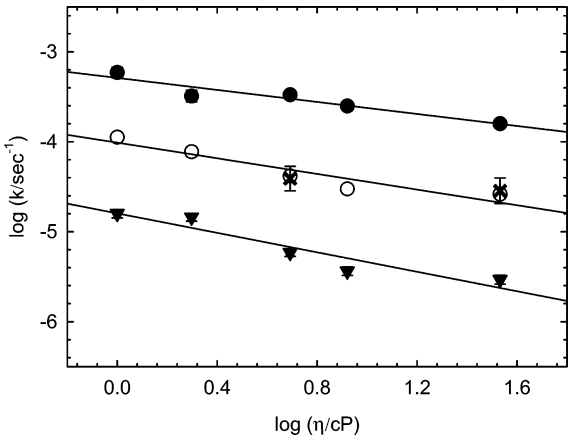

FIGURE 5: Viscosity dependence of relaxation rates on a log−log scale: (●) band III relaxation, process I; (○) band III relaxation, process II; (▼) band III relaxation, process III; and (×) 291 nm band relaxation. Error bars are shown. Solid lines are linear fits.

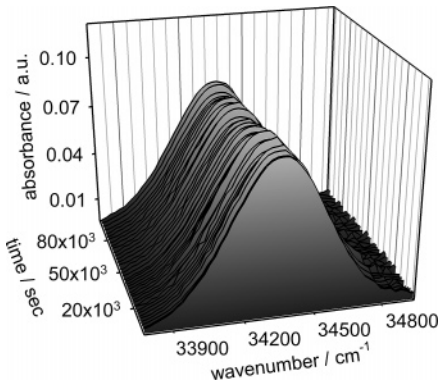

FIGURE 6: Time evolution of the near-UV band at ∼291 nm. The data are for a sample of HbO_2 encapsulated in a silica hydrogel; the co-encapsulated solvent is 40% (v/v) glycerol/water. T = 25 °C.

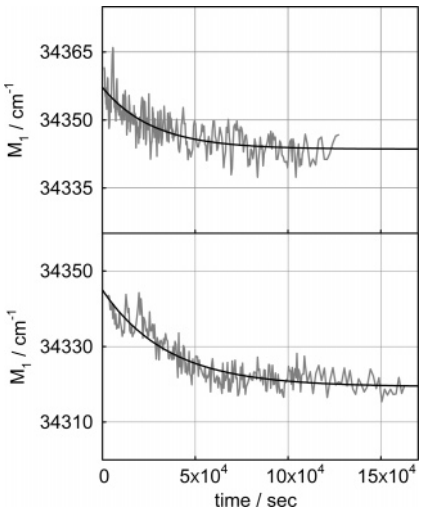

FIGURE 7: Time evolution of the first moment of the near-UV band. Solid lines are fittings with a single exponential: (top) 40% (v/v) glycerol/water and (bottom) 70% (v/v) glycerol/water.

Near-UV Spectral Relaxation. To elucidate the structural counterpart of the spectral relaxations monitored by band III, we performed experiments using as a spectral marker the Trpβ37 band in the near-UV region that probes the $\alpha_1\beta_2$ interface and in particular the formation of the Trpβ37−Aspα94 hydrogen bond in the hinge contact region characteristic of the T quaternary conformation. We have studied two samples of sol−gel-encapsulated HbO_2 having 40 and 70% glycerol/water as co-encapsulated solvent; data for the 40% glycerol/water sample are shown in Figure 6. Figure 7 reports the time dependence of the first moment of the band for both samples that were investigated; in the case of the near-UV band, no relevant M_0 and M_2 variations are observed in the time span of the experiment. As shown in Figure 7, a single exponential fits the data very well, implying that the relaxation of the Trpβ37 band monitors a single monophasic process. In analogy with the band III behavior, the characteristic time of this process markedly depends on solvent composition, as reported in Table 2. Since the two bands monitor different sites in the protein, it is remarkable that, for both 40 and 70% (v/v) glycerol/water, the characteristic times observed for the near-UV relaxation coincide with those relative to process II observed in the band III relaxation.

Table 2: Solvent Dependence of the Characteristic Time Observed in the Relaxation of the Near-UV Band at ∼291 nm

glycerol/water (v/v)	τ (s)
40%	$(25.7 \pm 3.5) \times 10^3$
70%	$(35.2 \pm 5.0) \times 10^3$

CONCLUSIONS

The time dependence of band III after deoxygenation of sol−gel encapsulated HbO_2 indicates the presence of three relaxation processes that we label, in order of increasing time constants, processes I, II, and III; since these effects are not observed for myoglobin, we attribute them to quaternary relaxations (the R → T transition) that drive the protein toward the deoxygenated equilibrium structure (T state). Only one of these events (the intermediate one, process II) has a counterpart in the near-UV Trpβ37 band and is simultaneous with the formation of the hinge contact Trpβ37−Aspα94 hydrogen bond that links the C helix of one α chain with the F helix of the opposite β chain and is characteristic of the quaternary T structure. This process in solution and at room temperature occurs 2−3 μs after photolysis of HbCO, as reported by Goldbeck et al. (*11*) and by Balakrishnan et al. (*12*); in sol−gel-encapsulated hemoglobin, it occurs ∼9 × 10^3 s after deoxygenation, implying that sol−gel encapsulation is able to reduce the rates of quaternary relaxations by more than 9 orders of magnitude. Moreover, our data suggest that the relaxation monitored by the near-UV Trpβ37 band and process II monitored by the near-IR band III reflect the same structural event and therefore that the structural deformation of the R-state $\alpha_1\beta_2$ interface necessary for the formation of the hinge contact hydrogen bond is transmitted to the heme environment; this is plausible since the H-bond formation described above involves the F helix to which the heme is linked and constitutes direct evidence that conformational changes at the $\alpha_1\beta_2$ interface are indeed transmitted to the heme environment, thus likely affecting the functional properties of the protein.

With regard to processes I and III monitored by band III, our data do not enable us to identify their structural origin. However, it would be tempting to speculate that both processes correspond to the relaxations observed in solution, both with transient optical absorption (*8*, *10*, *16*) and with transient UVRR (*12*) spectroscopy, at ∼750 ns and ∼20 μs, respectively. In a manner independent of any specific

assignment, our data support a multistep pathway for the R → T allosteric transition in hemoglobin.

Finally, we stress that all the observed relaxation rates depend markedly upon the composition of the solvent co-encapsulated within the matrix pores and decrease with an increase in solvent viscosity. This fact may be taken as an indication that quaternary relaxations in hemoglobin follow the α relaxation of the solvent, in agreement with the slaving hypothesis. This underlines the biological relevance of investigations of the dynamic properties of proteins and solvents in confined geometries and of the strict interplay between solvent and protein dynamics that may be enhanced by confinement and crowding. From an applicative point of view, these results suggest the possibility of controlling the rates of conformational changes of proteins immobilized within solid porous matrices by varying the viscosity of the co-encapsulated solvent.

ACKNOWLEDGMENT

We are indebted to Dr. Matteo Levantino and to Dr. Marco Cammarata for discussions and comments.

REFERENCES

1. Perutz, M. F. (1970) Stereochemistry of cooperative effects in haemoglobin, *Nature 228*, 726−739.
2. Shaanan, B. (1983) Structure of human oxyhaemoglobin at 2.1 Å resolution, *J. Mol. Biol. 171*, 31−59.
3. Fermi, G., Perutz, M. F., Shaanan, B., and Fourme, R. (1984) The crystal structure of human deoxyhaemoglobin at 1.74 Å resolution, *J. Mol. Biol. 175*, 159−174.
4. Silva, M. M., Rogers, P. H., and Arnone, A. (1992) A third quaternary structure of human hemoglobin A at 1.7-Å resolution, *J. Biol. Chem. 267*, 17248−17256.
5. Lukin, J. A., Kontaxis, G., Simplaceanu, V., Yuan, Y., Bax, A., and Ho, C. (2003) Quaternary structure of hemoglobin in solution, *Proc. Natl. Acad. Sci. U.S.A. 100*, 517−520.
6. Baldwin, J., and Chothia, C. (1979) Haemoglobin: The structural changes related to ligand binding and its allosteric mechanism, *J. Mol. Biol. 129*, 175−220.
7. Perutz, M. F., Wilkinson, A. J., Paoli, M., and Dodson, G. G. (1998) The stereochemical mechanism of the cooperative effects in hemoglobin revisited, *Annu. Rev. Biophys. Biomol. Struct. 27*, 1−34.
8. Jones, C. M., Ansari, A., Henry, E. R., Christoph, G. W., Hofrichter, J., and Eaton, W. A. (1992) Speed of intersubunit communication in proteins, *Biochemistry 31*, 6692−6702.
9. Björling, S. C., Goldbeck, R. A., Paquette, S. J., Milder, S. J., and Kliger, D. S. (1996) Allosteric intermediates in hemoglobin. 1. Nanosecond time-resolved circular dichroism spectroscopy, *Biochemistry 35*, 8619−8627.
10. Goldbeck, R. A., Paquette, S. J., Björling, S. C., and Kliger, D. S. (1996) Allosteric intermediates in hemoglobin. 2. Kinetic modeling of HbCO photolysis, *Biochemistry 35*, 8628−8639.
11. Goldbeck, R. A., Esquerra, R. M., and Kliger, D. S. (2002) Hydrogen bonding to Trp β37 is the first step in a compound pathway for hemoglobin allostery, *J. Am. Chem. Soc. 124*, 7646−7647.
12. Balakrishnan, G., Tsai, C. H., Wu, Q., Case, M. A., Pevsner, A., McLendon, G. L., Ho, C., and Spiro, T. G. (2004) Hemoglobin site-mutants reveal dynamical role of interhelical H-bonds in the allosteric pathway: Time-resolved UV resonance Raman evidence for intra-dimer coupling, *J. Mol. Biol. 340*, 857−868.
13. Balakrishnan, G., Case, M. A., Pevsner, A., Zhao, X., Tengroth, C., McLendon, G. L., and Spiro, T. G. (2004) Time-resolved absorption and UV resonance Raman spectra reveal stepwise formation of T quaternary contacts in the allosteric pathway of hemoglobin, *J. Mol. Biol. 340*, 843−856.
14. Mouawad, L., Perahia, D., Robert, C. H., and Guilbert, C. (2002) New insights into the allosteric mechanism of human hemoglobin from molecular dynamics simulations, *Biophys. J. 82*, 3224−3245.
15. Xu, C., Tobi, D., and Bahar, I. (2003) Allosteric changes in protein structure computed by a simple mechanical model: Hemoglobin T↔R2 transition, *J. Mol. Biol. 333*, 153−168.
16. Hofrichter, J., Sommer, J. H., Henry, E. R., and Eaton, W. A. (1983) Nanosecond absorption spectroscopy of hemoglobin: Elementary processes in kinetic cooperativity, *Proc. Natl. Acad. Sci. U.S.A. 80*, 2235−2239.
17. Henry, E. R., Jones, C. M., Hofrichter, J., and Eaton, W. A. (1997) Can a two state MWC allosteric model explain hemoglobin kinetics? *Biochemistry 36*, 6511−6528.
18. Henry, E. R., Bettati, S., Hofrichter, J., and Eaton, W. A. (2002) A tertiary two-state allosteric model for hemoglobin, *Biophys. Chem. 98*, 149−164.
19. Colombo, M. F., Rau, D. C., and Parsegian, V. A. (1992) Protein solvation in allosteric regulation: A water effect in hemoglobin, *Science 256*, 655−659.
20. Bulone, D., SanBiagio, P. L., Palma-Vittorelli, M. B., and Palma, M. U. (1993) The role of water in hemoglobin function and stability, *Science 259*, 1335−1336.
21. Cordone, L., Cupane, A., SanBiagio, P. L., and Vitrano, E. (1981) Effect of some organic cosolvents on the reaction of hemoglobin with oxygen, *Biopolymers 20*, 39−51.
22. Bulone, D., Cupane, A., and Cordone, L. (1983) Conformational and functional properties of hemoglobin in water-organic cosolvents mixtures: The effect of ethylene glycol and glycerol on the oxygen affinity, *Biopolymers 22*, 119−123.
23. Ansari, A., Jones, C. M., Henry, E. R., Hofrichter, J., and Eaton, W. A. (1992) The role of solvent viscosity in the dynamics of protein conformational changes, *Science 256*, 1796−1798.
24. Goldbeck, R. A., Paquette, S. J., and Kliger, D. S. (2001) The effect of water on the rate of conformational change in protein allostery, *Biophys. J. 81*, 2919−2934.
25. Fenimore, P. W., Frauenfelder, H., McMahon, B. H., and Parak, F. G. (2002) Slaving: Solvent fluctuations dominate protein dynamics and function, *Proc. Natl. Acad. Sci. U.S.A. 99*, 16047−16051.
26. Sawicki, C. A., and Gibson, Q. H. (1976) Quaternary conformational changes in human hemoglobin studied by laser photolysis of carboxyhemoglobin, *J. Biol. Chem. 251*, 1533−1542.
27. Friedman, J. M. (1985) Structure, dynamics, and reactivity in hemoglobin, *Science 228*, 1273−1280.
28. Findsen, E. W., Friedman, J. M., Ondrias, M. R., and Simon, S. R. (1985) Picosecond time-resolved resonance Raman studies of hemoglobin: Implications for reactivity, *Science 229*, 661−665.
29. Chen, R., and Spiro, T. G. (2002) Monitoring the allosteric transition and CO rebinding in hemoglobin with time-resolved FTIR spectroscopy, *J. Phys. Chem. A 106*, 3413−3419.
30. Hu, X., Rodgers, K. R., Mukerji, I., and Spiro, T. G. (1999) New light on allostery: Dynamic resonance Raman spectroscopy of hemoglobin Kempsey, *Biochemistry 38*, 3462−3467.
31. Vitale, D. J., Goldbeck, R. A., Kim-Shapiro, D. B., Esquerra, R. M., Parkhurst, L. J., and Kliger, D. S. (2000) Near-ultraviolet magnetic circular dichroism spectroscopy of protein conformational states: Correlation of tryptophan band position and intensity with hemoglobin allostery, *Biochemistry 39*, 7145−7152.
32. Ellerby, L. M., Nishida, C. R., Nishida, F., Yamanaka, S. A., Dunn, B., Valentine, J. S., and Zink, J. I. (1992) Encapsulation of proteins in transparent porous silicate glasses prepared by the sol-gel method, *Science 255*, 1113−1115.
33. Shibayama, N., and Saigo, S. (1995) Fixation of the quaternary structures of human adult haemoglobin by encapsulation in transparent porous silica gels, *J. Mol. Biol. 251*, 203−209.
34. Schirò, G., Cammarata, M., Levantino, M., and Cupane, A. (2005) Spectroscopic markers of the T→R transition in human hemoglobin, *Biophys. Chem. 114*, 27−33.
35. Shibayama, N., and Saigo, S. (1999) Kinetics of the allosteric transition in hemoglobin within silicate sol-gels, *J. Am. Chem. Soc. 121*, 444−445.
36. Shibayama, N. (1999) Functional analysis of hemoglobin molecules locked in doubly liganded conformations, *J. Mol. Biol. 285*, 1383−1388.
37. Khan, I., Shannon, C. F., Dantsker, D., Friedman, A. J., Perez-Gonzalez-de-Apodaca, J., and Friedman, J. M. (2000) Sol-gel trapping of functional intermediates of hemoglobin: Geminate and bimolecular recombination studies, *Biochemistry 39*, 16099−16109.
38. Das, T. K., Khan, I., Rousseau, D. L., and Friedman, J. L. (1999) Temperature dependent quaternary state relaxation in sol-gel encapsulated hemoglobin, *Biospectroscopy 5*, S64−S70.

39. Samuni, U., Dantsker, D., Khan, I., Friedman, A. J., Peterson, E., and Friedman, J. M. (2002) Spectroscopically and kinetically distinct conformational populations of sol-gel encapsulated carbonmonoxy myoglobin: A comparison with hemoglobin, *J. Biol. Chem. 277*, 25783−25790.
40. Eaton, W. A., Hanson, L. K., Stephens, P. J., Sutherland, J. C., and Dunn, J. B. R. (1978) Optical spectra of oxy- and deoxyhemoglobin, *J. Am. Chem. Soc. 100*, 4991−5003.
41. Sassaroli, M., and Rousseau, D. L. (1987) Time dependence of near-infrared spectra of photodissociated hemoglobin and myoglobin, *Biochemistry 26*, 3092−3098.
42. Chavez, M. D., Courtney, S. H., Chance, M. R., Kiula, D., Nocek, J., Hoffman, B. M., Friedman, J. M., and Ondrias, M. R. (1990) Structural and functional significance of inhomogeneous line broadening of band III in hemoglobin and Fe-Mn hybrid hemoglobins, *Biochemistry 29*, 4844−4852.
43. Huang, J., Ridsdale, A., Wang, J., and Friedman, J. M. (1997) Kinetic hole burning, hole filling, and conformational relaxation in heme proteins: Direct evidence for the functional significance of a hierarchy of dynamical processes, *Biochemistry 36*, 14353−14365.
44. Perutz, M. F., Ladner, E. J., Simon, S. R., and Ho, C. (1974) Influence of globin structure on the state of the heme. I. Human deoxyhemoglobin, *Biochemistry 13*, 2163−2173.
45. Perutz, M. F., Fersht, A. R., Simon, S. R., and Roberts, G. C. (1974) Influence of globin structure on the state of the heme. II. Allosteric transitions in methemoglobin, *Biochemistry 13*, 2174−2186.
46. Peterson, E. S., and Friedman, J. M. (1998) A possible allosteric communication pathway identified through a resonance Raman study of four β37 mutants of human hemoglobin A, *Biochemistry 37*, 4346−4357.
47. Kiger, L., Klinger, A. L., Kwiatkowski, L. D., De Young, A., Doyle, M. L., Holt, J. M., Noble, R. W., and Ackers, G. K. (1998) Thermodynamic studies on the equilibrium properties of a series of recombinant βW37 hemoglobin mutants, *Biochemistry 37*, 4336−4345.
48. Cordone, L., Cupane, A., San Biagio, P. L., and Vitrano, E. (1979) Effect of some monohydric alcohols on the oxygen affinity of hemoglobin: Relevance of solvent dielectric constant and hydrophobicity, *Biopolymers 18*, 1975−1988.
49. Hayashi, Y., Puzenko, A., and Feldman, Y. (2006) Slow and fast dynamics in glycerol-water mixtures, *J. Non-Cryst. Solids 352*, 4696−4703.
50. Wei, Y., Xu, J., Feng, Q., Dong, H., and Lin, M. (2000) Encapsulation of enzymes in mesoporous host materials via the nonsurfactant-templated sol-gel process, *Mater. Lett. 44*, 6−11.
51. Wei, Y., Dong, H., Xu, J., and Feng, Q. (2002) Simultaneous immobilization of horseradish peroxidase and glucose oxidase in mesoporous sol-gel host materials, *ChemPhysChem 3*, 802−808.
52. Steinbach, P. J. (2002) Inferring lifetime distributions from kinetics by maximizing entropy using a bootstrapped model, *J. Chem. Inf. Comput. Sci. 42*, 1476−1478.
53. Steinbach, P. J., Ionescu, R., and Matthews, C. R. (2002) Analysis of kinetics using a hybrid maximum-entropy/nonlinear-least-squares method: Application to protein folding, *Biophys. J. 82*, 2244−2255.
54. Lim, M., Jackson, T. A., and Anfinrud, P. A. (1993) Nonexponential protein relaxation: Dynamics of conformational change in myoglobin, *Proc. Natl. Acad. Sci. U.S.A. 90*, 5801−5804.
55. Franzen, S., and Boxer, S. G. (1997) On the origin of heme absorption band shifts and associated protein structural relaxation in myoglobin following flash-photolysis, *J. Biol. Chem. 272*, 9655−9660.
56. Stavrov, S. S. (2001) Optical absorption band III of deoxyheme proteins as a probe of their structure and dynamics, *Chem. Phys. 271*, 145−154.
57. Srajer, V., and Champion, P. M. (1991) Investigations of optical line shapes and kinetic hole burning in myoglobin, *Biochemistry 30*, 7390−7402.
58. Yedgar, S., Tetreau, C., Gavish, B., and Lavalette, D. (1995) Viscosity dependence of O_2 escape from respiratory proteins as a function of cosolvent molecular weight, *Biophys. J. 68*, 665−670.
59. Frauenfelder, H., Fenimore, P. W., Chen, G., and McMahon, B. H. (2006) Protein folding is slaved to solvent motions, *Proc. Natl. Acad. Sci. U.S.A. 103*, 15469−15472.
60. Fenimore, P. W., Frauenfelder, H., McMahon, B. H., and Young, R. D. (2004) Bulk-solvent and hydration-shell fluctuations, similar to α and β fluctuations in glasses, control protein motions and functions, *Proc. Natl. Acad. Sci. U.S.A. 101*, 14408−14413.
61. Lubchenko, V., Wolynes, P. G., and Frauenfelder, H. (2005) Mosaic energy landscapes of liquids and the control of protein conformational dynamics by glass-forming solvents, *J. Phys. Chem. B 109*, 7488−7499.
62. Timasheff, S. N. (2002) Protein hydration, thermodynamic binding and preferential hydration, *Biochemistry 41*, 13473−13482.

BI701166M